SULFUR SOLUBILITY IN SILICATE MELTS UNDER HIGHLY REDUCING CONDITIONS RELEVANT TO MERCURY. K. E. Vander Kaaden and F. M. McCubbin, Institute of Meteoritics, 1 University of New Mexico, MSC03-2050, Albuquerque, NM 87131, (kvander@unm.edu).

Introduction: Results from the MErcury **S**urface, Space ENvironment, GEochemistry, and Ranging (MESSENGER) spacecraft show the surface of Mercury has high S abundances (~4 wt%) and low FeO abundances (<2 wt%) [1-3]. Based on the Fe abundance, the oxygen fugacity of Mercury's surface materials was estimated to be approximately 3 $\log_{10}$ units below the IW buffer (ΔIW-3) [4]. McCubbin et al. [5] compiled sulfur solubility data from numerous studies [6-12] and demonstrated that sulfur solubility in silicate melts increases with decreasing oxygen fugacity, and estimated that the S abundances of Mercury's surface were consistent with fO_2's as low as ΔIW-5. Other studies have pushed the range to even lower values [ΔIW-7; 13].

Much of our geochemical understanding of elements in natural systems comes from empirical observations of terrestrial rocks and other planetary bodies, which may not apply to a planet as reduced as Mercury. Consequently, any broad geochemical interpretations that are rooted in these empirical observations may be misguided. In fact, interpretations of magmatic processes on Mercury are difficult at present because the numbers of experimental studies relevant to the extremely low fO_2 and high sulfur content of Mercury are very limited. At such reducing conditions, elements are likely to deviate from their typical geochemical behavior displayed at higher oxygen fugacity. The goal of our current study is to investigate S contents of silicate liquids at sulfide saturation (SCSS) in silicate magmas as a function of pressure, temperature, and oxygen fugacity. Our investigation begins by using the composition of the northern volcanic plains lavas which are smooth plains covering 6% of the surface area of Mercury and are less cratered than their surroundings, suggesting they are volcanic in origin [14]. These lavas are the most likely example of a lava that can be compositionally assessed from orbit making them the best candidate to study S solubility experimentally. From these experiments, we hope to gain a better understanding of the role of S in mercurian magmas.

Methods: Experiments were conducted at 0.5 and 1 GPa from 1300 °C to 1600 °C using a 13 mm piston cylinder apparatus and a salt-pyrex cell. Experiments at 4 GPa were conducted in a Walker-style multi anvil device from 1750 °C to 2050 °C. Run durations ranged from 2-24 hours depending on the stability of the cell assembly. All experiments were run in graphite capsules to minimize interaction between capsule material and the sulfur-bearing starting materials. Each experiment was set up by first packing Si-metal, FeS, and the NVP silicate starting material or diopside starting material (Table 1) into the capsule in an ~ 2:2:3 mixture. The Si-metal was added to each capsule in order to reduce the oxygen fugacity of the experiment to mercurian conditions and allow the S to dissolve into the silicate melt. All run products were polished using hexagonal boron nitride powder instead of water to ensure no sulfide phases were lost from the experimental charges [15]. All phases, including silicate glass, metals, and sulfides, were analyzed using a JEOL 8200 superprobe at the University of New Mexico. Oxygen fugacity was calculated relative to the IW buffer and secondarily checked against the Si-SiO_2 buffer.

Table 1. Composition of the silicate starting materials used in this study. Average NVP composition from [1, 3, 16, 17].

	Average NVP	Alkali- and Sulfur-Bearing	Diopside
SiO_2	56.07	54.05	55.49
TiO_2	0.81	1.26	-------
Al_2O_3	13.67	12.60	-------
Cr_2O_3	0.77	0.74	-------
FeO	1.01	-------	-------
MgO	15.21	14.25	18.61
MnO	0.68	0.65	-------
CaO	4.11	5.23	25.90
Na_2O	7.00	6.81	-------
K_2O	0.22	0.25	-------
FeS	0	4.16	-------
S	0.92	-------	-------
$^-$O=S	0.47	-------	-------
Total	100.00	100.00	100.00

Results: The addition of Si-metal to each experimental charge reduced the oxygen fugacity of these experiments to a range between ΔIW-6.8 and ΔIW-3.8. The SCSS in all experimental charges ranged from 1.16 wt% S to 16.70 wt% S. These experimental results are shown in Figure 1 in comparison to previously published data [6-12]. Including data from [11] for all pressures (0.0001-4 GPa), SCSS increases with increasing temperature (Figure 2A). However, the slope of this variation differs with pressure. At 0.0001 GPa (1 bar), the slope is -26.9 and increases to -140.5 at 4 GPa. Similarly, for our only overlapping

temperature (1400 °C), SCSS increases with increasing pressure, at least between 0.5 and 1 GPa (Figure 2B).

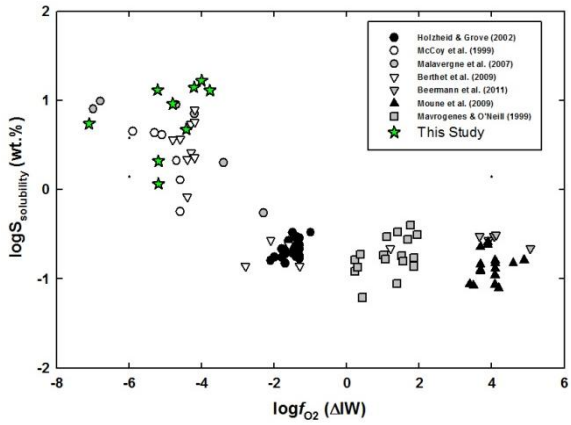

Figure 1. Log_{10} SCSS vs. log_{10} fO_2 relative to the iron-wüstite buffer. Figure adapted from [5].

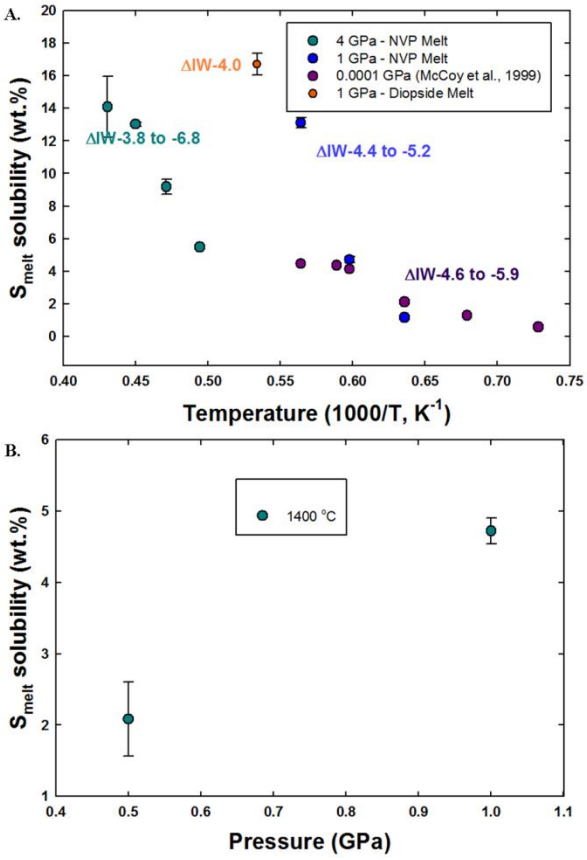

Figure 2. SCSS (wt%) in silicate melt as a function of temperature (A) and pressure (B).

Discussion: The slope of the temperature effect on SCSS varies as a function of pressure. However, the slope of the temperature effect on SCSS at 1 GPa and 4 GPa is much steeper than the 0.0001 GPa data from [11]. In addition, the slope of the temperature effect on SCSS is very similar for the 1 GPa and 4 GPa data. Additional experimental data are needed between 0.0001 and 1 GPa to assess the effect of pressure on SCSS.

Although SCSS increases as a function of temperature at all pressures, the temperature effect on SCSS correlates more strongly with the amount of super-heating above the liquidus temperature rather than absolute temperature. This point is illustrated in Figure 2A where lower temperature melts at 1 GPa have higher SCSS values than higher temperature melts at 4 GPa, but both sets of experiments display similar increasing trends in SCSS as a function of T. We interpret this behavior to indicate that silicate melt structure, or melt viscosity, may also play a role in controlling SCSS at these reducing conditions. Although we did not closely examine the effect of melt composition on SCSS, we conducted a single experiment on a diopside melt composition (Table 1) at 1 GPa which falls on the extension for the slope of the corresponding 1 GPa data on the NVP melt composition, so melt composition may play a subordinate role on SCSS to temperature.

These results indicate that the elevated abundances of sulfur on Mercury's surface can be explained by transport within highly reduced silicate magmas, which have a much higher carrying capacity for sulfur than moderately reduced to oxidizing magmas. In addition to oxygen fugacity, both pressure and temperature will have a strong effect on the carrying capacity of silicate melts during partial melting in Mercury's interior. In order to determine the role of viscosity on sulfur solubility we are beginning to investigate much simpler silicate systems including pure SiO_2 melt as well as a diopside ($CaMgSi_2O_6$) melt.

References: [1] Nittler, L.R., et al., (2011) *Science*, **333**(6051): p. 1847-1850. [2] Peplowski, P.N., et al., (2012) *JGR - Planets*, **117**(E00L04). [3] Weider, S.Z., et al., (2012) *JGR - Planets*, **117**(E00L05). [4] Zolotov, M.Y., et al. (2011) in *EOS (Transactions, American Geophysical Union)*. San Francisco, CA: AGU. [5] McCubbin, F.M., et al., (2012) *GRL*, **39**. [6] Beermann, O., et al., (2011) *GCA*, **75**(23): p. 7612-7631. [7] Berthet, S., V. Malavergne, and K. Righter, (2009) *GCA*, **73**(20): p. 6402-6420. [8] Holzheid, A. and T.L. Grove, (2002) *AmMin*, **87**(2-3): p. 227-237. [9] Malavergne, V., S. Berthet, and K. Righter. (2007) *38th LPSC*. Houston, TX: LPI. [10] Mavrogenes, J.A. and H.S.C. O'Neill, (1999) *GCA*, **63**(7-8): p. 1173-1180. [11] McCoy, T.J., T.L. Dickinson, and G.E. Lofgren, (1999) *MAPS*, **34**(5): p. 735-746. [12] Moune, S., F. Holtz, and R.E. Botcharnikov, (2009) *Contribs Min Pet*, **157**(6): p. 691-707. [13] Zolotov, M.Y., et al., (2013) *JGR-Planets*, **118**(1). [14] Head, J.W., et al., *(*2011*) Science*, **333**(6051): p. 1853-1856. [15] Murthy, V.M., W. van Westrenen, and Y.W. Fei, *(*2003*) Nature*, **423**(6936): p. 163-165. [16] Peplowski, P.N., et al., *(*2014*) Icarus* **228**: 86-95. [17] Evans, L.G., et al., *(*2013*) 44th LPSC*. The Woodlands, TX. p. # 2033.